Mahdi Shahparasti, Joan Rocabert, Raul Santiago Muñoz, Alvaro Luna, Pedro Rodríguez. (2018) Impedance source interlinking converter for microbial electrosynthesis energy storage applications. *7th International Conference on Renewable Energy Research and Applications: Paris, France, Oct. 14-17, 2018* : IEEE, 2018. Pp. 1340-1345 Doi: 10.1109/ICRERA.2018.8566712.

Mahdi Shahparasti, Joan Rocabert, Raul Santiago Muñoz, Alvaro Luna, Pedro Rodríguez. (2018) Impedance source interlinking converter for microbial electrosynthesis energy storage applications. *7th International Conference on Renewable Energy Research and Applications: Paris, France, Oct. 14-17, 2018* : IEEE, 2018. Pp. 1340-1345 Doi: 10.1109/ICRERA.2018.8566712.

Impedance Source Interlinking Converter for Microbial Electrosynthesis Energy Storage Applications

Mahdi Shahparasti[1], Joan Rocabert[1], Raul Santiago Muñoz[1], Alvaro Luna[1], Pedro Rodríguez[1,2]
[1] Department of Electrical Engineering, Technical University of Catalonia, 08222 Barcelona, Spain
[2] Loyola Tech, University of Loyola Andalucia, 41014 Sevilla, Spain
Mahdi.shahparasti@upc.edu

***Abstract*— In this paper, a new type of single-stage interlinking converters for Microbial Electrosynthesis (MES) energy storage applications connected to the three-phase grid is presented, in which impedance source network (ZSN) is employed to reduce cost and volume, and meanwhile improve the efficiency. Impedance source converter (ISC) with buck-boost characteristic is able to feed MES with a wide range of voltages in DC side, also, converter grid distortion in AC side is reduced because there is no need to dead time for switching. Different ZSNs are studied and discussed for MES energy application. The applicable ones are selected and a comprehensive comparison is presented. Also, the proposed efficient control for ISC consists of two parts, first ZSN capacitor control plus reactive power control are done by controlling modulation index, and second the objective of tracking active power reference can be achieved by means of controlling shoot-through duty cycle. Simulation results are presented to certify the comparison between ZSNs and to verify the merit of the proposed control scheme.**

Keywords*— *Interlinking converter; Microbial Electrosynthesis; impedance source network; Power converter.

I. INTRODUCTION

Today, using of renewable energy sources has been increased due to fossil fuels high costs and their harmful influences on the environment [1-2], therefore, the high penetration of renewable energy resources lead to new challenges in power system because of their variability [3-4]. Some of these challenges are listed here such as accurate forecasting, voltage control, energy storages management, demand management system, and power system stability [5-6].To keep the grid supply and demand in balance, the large-capacity and long-term electricity storage is needed, also reserve production capacity[7-8]. The Power-to-Gas (P2G) especially Power-to- Methane technology can contribute to tackle this issue [9-10]. The P2G links the electricity sector with the gas grid by converting electrical power into a grid-compatible gas [11-12]. New improvements make the MES more realistic and therefore requires the development of a process control system [13]. In current technology, for achieving a controllable energy storage, the MES stack has to be supplied with variable DC voltage. Therefore, to feed MES stack with wide voltage range, a two stage interlinking converter (IC) consists of two level voltage source plus DC/DC buck converter must be used to connect three phase grid to MES stack.

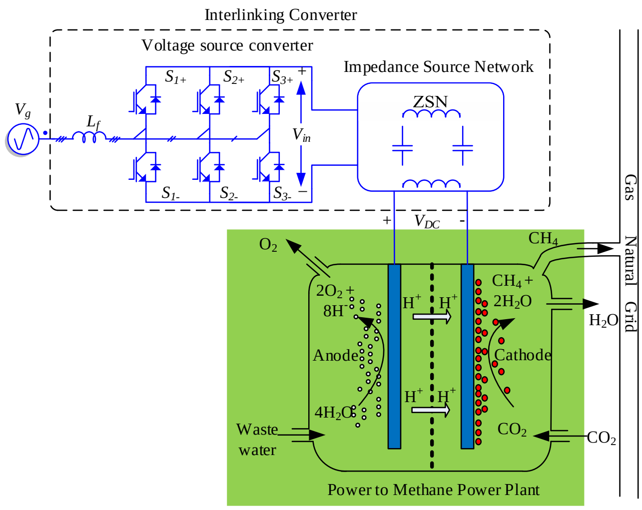

Fig. 1. Impedance Source Interlinking Converter for Microbial Electrosynthesis Energy Storage Applications.

Since the introduction of Z-source converter, many kinds of research have been done to use impedance source converters as a single stage power conditioner converter for different applications such as PV systems, wind systems, motor drive,…[14]. In this paper, for first time, according to Fig1, impedance source converters are proposed as P2G interlinking converter due to the following advantages: (1) ability for supplying MES with wide of voltage, (2) plug-and-play capability, (3) avoid using dead time for switching and improvement of the power quality.

This paper is organized as follows. Microbial electrosynthesis energy storage is briefly introduced in section II. In Sections III, the description of the proposed ISC topology and its control system are presented. In Section IV, the simulation results and comparative assessment that permits to investigate the performance of the proposed controller are presented. Finally, the conclusions that arise from this work are presented in Section IV.

II. Microbial ElectroSynthesis Energy Storage

Microbial electrosynthesis (MES) is a form of microbial electrocatalysis in which electrons are supplied to living microorganisms by applying a DC voltage to the stack [15]. The electrons are then used by the microorganisms to reduce carbon dioxide to yield methane and clean water from wastewater:

$$CO_2 + 8H^+ + 8e^- \rightarrow CH_4 + 2H_2O, \quad (1)$$

Waste streams from biorefineries e.g. bioethanol and biodiesel plants and wastewaters are candidate substrates for MES. MES integration helps biorefineries achieving the full polygeneration potentials, i.e. recovery of metals turning apparently pollutants from biorefineries into resources, creation of chemicals and biofuels from reprocess of CO2 and clean water [16]. Also, the produced methane can be transferred to natural gas distribution utility and there is not any difficulty related to gas storage.

III. Proposed ISC Topology

A. Overall System Configuration

ISC, see Fig.1, consists of a ZSN and full-bridge inverter (S1-S6). The ZSN can compose of capacitors, inductors, semiconductors and impulse transformers, which connects to the DC side of the inverter. Fig.2 shows two main structures of ZSN family which are analyzed in this paper.

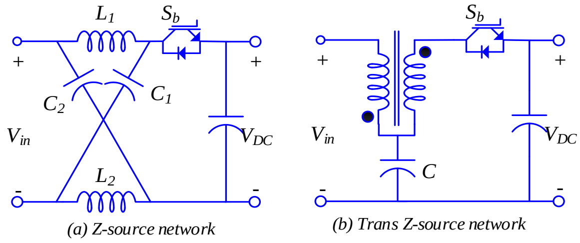

Fig. 2. Impedance Source Network family.

Conventional VSI has eight switching states including six active states and two zero states, but in ISC one extra zero state for bucking/boosting voltage joined these states that is called shoot-through state (vector). During shoot-through state DC link terminal (V_{in}) is shorted through by inverter bridge. Shoot-through state provides bucking capability for ISC and additional, it doesn't have to have dead time for switching. For ISC, the following relationship can be written for V_{DC}:

$$V_{DC} = b\frac{2V_{ac}}{M} \quad (2)$$

where b is buck factor and it can change between 0 and 1. V_{ac} is peak voltage of the grid. The value of b is determined by short-through time interval and adds a new degree of freedom to the system. Also, M is the modulation index. Fig.3 shows the proposed swathing pattern for ISC. In this method, two extra lines (V_p, $-V_p$) are used as shoot-through signals which result a shoot-through state for the ISC when the carrier is bigger than V_p or smaller that – V_p. The value M is related the peak of sinusoidal reference in Fig.3.

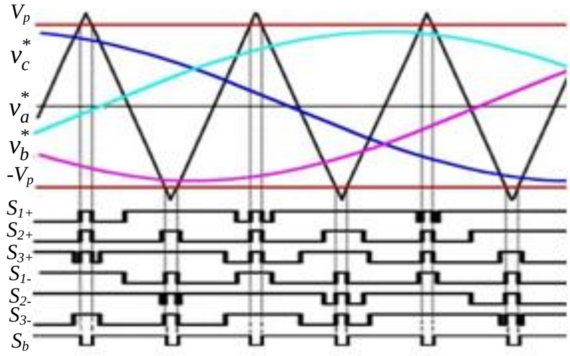

Fig. 3. Proposed switching pattern for ISC

B. ZSN operation principle

A Z-source network (Z-SN) is utilized to explore the operating principle of ZSCs. The circuit diagram of the equivalent circuit of Z-SN during active and shoot-through states are shown in Fig. 4.

During the shoot-through state, the input of Z-source network is short-circuited by switches of Inverter Bridge, and switch S_b in Z-SN is turned off and its body diode reverse biased (see Fig. 4-a). Energy of inductors transferred to capacitors during this shoot-through state:

$$\begin{aligned} V_{in} &= 0, \\ V_{L1} &= -V_{C1}, \\ V_{L2} &= -V_{C2}, \end{aligned} \quad (3)$$

During no shoot-through states, as shown in Fig. 4-b, switch S_b turns on and energy is transferred to the load. The switching circuit viewed from the dc side is modelled as a current source during the no shoot-through states.

$$\begin{aligned} V_{DC} &= V_{C1} + V_{C2} - V_{in}, \\ V_{L1} &= V_{in} - V_{C1}. \end{aligned} \quad (4)$$

Assuming that the inductors and capacitors of Z-source network have the same inductance and capacitance, respectively. Then, Z-source network becomes symmetrical. Given that the shoot-through state interval is T_0 during a switching cycle T_s, the average voltage of the inductors over one switching period should be zero in steady state, from (3) and (4), thus, it is found that,

$$\begin{aligned} &\langle V_{L1} \rangle = -V_{C1}T_0 + (T_s - T_0)(V_{in} - V_{C1}) = 0 \\ &\xrightarrow[D_0 = T_0/T_s]{} V_{C1} = V_{C2} = (1 - D_0)V_{in}, \end{aligned} \quad (5)$$

where D_0 is duty cycle of shoot-through state. The average value of output voltage can be found by substituting (5) into (4):

$$V_{DC} = \underbrace{(1 - 2D_0)}_{b} V_{in},. \quad (6)$$

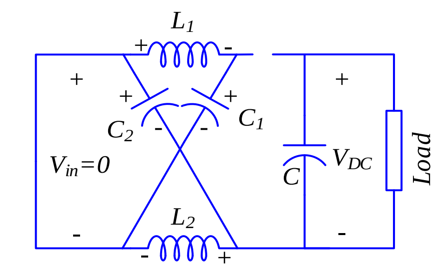

(a)

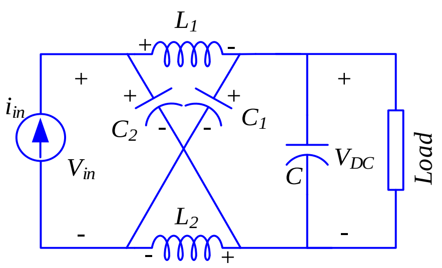

(b)

Fig. 4. Equivalent circuit of the Z-source network. (a) shoot-through state, (b) non shoot-through states.

For Trans Z-source network, the equivalent circuits during working states are shown in Fig. 5, the magnetizing inductance of the transformer is shown as L_m. In the shoot-through state, the energy of magnetizing inductor transferred to the capacitor (see Fig. 5-a):

$$\begin{aligned} V_{in} &= 0, \\ V_{Lm} &= -V_C, \end{aligned} \tag{7}$$

Also, during non-shoot-through states according to Fig. 5–b:

$$\begin{aligned} V_{DC} &= (1+n)V_C - nV_{in}, \\ V_{Lm} &= V_{in} - V_C. \end{aligned} \tag{8}$$

To prevent transformer saturation, the average voltage of magnetizing inductor over one switching period should be zero in steady state, hence,

$$\begin{aligned} &\langle V_{Lm} \rangle = -V_C T_0 + (T_s - T_0)(V_{in} - V_C) = 0 \\ &\xrightarrow[D_0 = T_0/T_s]{} V_C = (1 - D_0)V_{in}, \end{aligned} \tag{9}$$

The average value of load voltage can be found as follows:

$$V_{DC} = (1+n)V_C - nV_{in} = \underbrace{(1-(1+n)D_0)}_{b}V_{in}, \tag{10}$$

The main advantage of Trans Z-SN rather than Z-SN is that according to (6) and (10), with suitable selection of transformer turn ratio, the range of buck factor b increases for a specific shoot-through duty cycle.

To change the buck factor in the closed loop system, the value of V_p is selected as follows:

$$V_p = 1 - D_0, \tag{11}$$

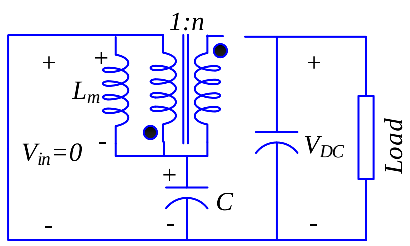

(a)

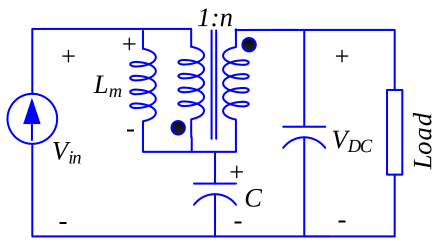

(b)

Fig. 5. Equivalent circuit of the Trans Z-SN. (a) shoot-through state, (b) non shoot-through states.

C. Proposed Control Scheme

The proposed control scheme is shown in Fig. 6. It is composed of two parts: 1) control of reactive power delivered to the grid and grid current, and 2) control of active power delivered to the MES stack. In this scheme, capacitor voltage of ZSN is kept constant around a specific value. As a result, if the capacitor voltage is controlled at a constant value, V_{DC} (active power delivered to MES) can be controlled by adjusting the shoot-through duty cycle.

Part 1of Control Scheme: The current reference in the stationary reference frame is found based on the output of ZSN capacitor voltage's PI controller, reactive power reference Q^* and the grid voltage [17]. The instantaneous power relationships in the synchronous reference frame (SRF) are given by:

$$P = \frac{3}{2}\left(V_{dg} i_d + V_{qg} i_q\right) \tag{12}$$

$$Q = \frac{3}{2}\left(V_{qg} i_d + V_{dg} i_q\right) \tag{13}$$

where P and Q are active power and reactive power, respectively, i is the grid current, and V_g is the grid voltage. The subscripts "q" and "d" is used to refer to quadrature and direct components, respectively. If the reference frame is oriented along the grid voltage, V_{qg} will be equal to zero. Then, active and reactive power control can be realized by controlling direct and quadrature current components, respectively [18]. Here, the current reference in d axis i_d^* is equal to the output of capacitor voltage controller, and in q axis i_q^* can be found as follows:

$$i_q^* = \frac{2Q^*}{3V_{dg}} \tag{14}$$

Then, the current reference in natural reference frame i_{abc}^* is obtained with inverse park transformation of i_d^* and i_q^*. A proportional-resonant (PR) controller is employed to track current reference with zero steady-state error and a fast dynamic response.

$$PR = K_p + \sum_{h=1,3,5,...}^{odd} \frac{2K_{ih}\omega_{ch}s}{s^2 + 2\omega_{ch}s + h^2\omega_o^2} \quad (15)$$

where h, K_p, K_{ih}, ω_o and ω_{ch} are harmonic order, the proportional coefficient, the resonant coefficients, the resonant frequency and the resonant bandwidths, respectively.

Part2 of Control Scheme: Regarding (16), if the capacitor voltage of the ZSN 'V_C' is controlled around a constant value, the input voltage of MES decreases as the shoot-through state duty cycle increases. This can be seen in Fig. 7 for different n ratios.

$$V_{dc} = \frac{1-(n+1).D_0}{1-D_0} V_C \quad (16)$$

As a result, if the capacitor voltage is controlled at a constant value, V_{dc} can be controlled by adjusting the shoot-through duty cycle. Therefore, active power control can be realized by controlling the shoot-through duty cycle. The active power control method is shown in Fig. 6, the voltage and current of a MES are used for active power calculation ($V_{dc}*I_{MES}$) and the shoot-through reference signal V_p is equal to the output of PI controller in the power loop.

In fact in Fig. 6, v_{abc}^* is equal to the output of PR controller. In another side, V_p is determined based on the active power control loop.

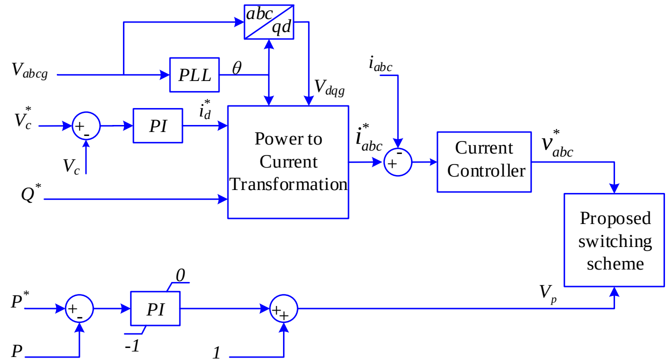

Fig. 6. Proposed control scheme.

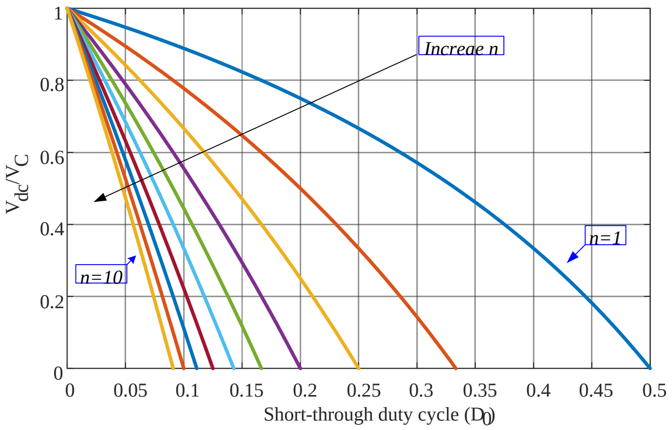

Fig. 7. Output voltage v.s capacitor voltage of ZSN based on the shoot-through duty cycle and transformer turn ratio.

IV. Simulation

To validate the performance of the proposed control method and also the comparison between ICs, an 8kW MES stack with ISC interlinking converters is simulated. The grid voltage and frequency are 380V and 50 Hz, respectively. The parameters of ICs (Z-source converter and Trans Z-source converter) are listed in Table 1.

According to [19], MES stack has a very slow dynamic and its time constant is around several hours. Therefore, it is modeled as an equivalent resistor with curve fitting of available data.

Table 1 Simulation parameters.

Parameter	Value
Grid voltage	380V-50Hz
Grid short circuit capacity (SCC)	10kA
Nominal power	8kVA
Grid side filter (L_f)	3 mH
Switching frequency	10kHz
DC link capacitor (C)	2200 µF
ZSC inductors (L_1, L_2)	1 mH
ZSC capacitors (C_1, C_2)	220 µF
Magnetizing inductance of transformer of Trans ZSC (L_m)	2 mH
Trans ZSC capacitor (C)	330 µF

A. Simulation of Proposed System

The plots in the section gather the obtained results where Q^* is set to 0 and P^* changes from 8000W, to 6000 at t = 2 s, then to 4000W at t=3 s, finally to 8000W at t=4s.

The current and voltage of the grid, for both ISC are the same, and they are shown in Fig. 8 where the grid current is sinusoidal. The total harmonic distortion (THD) of grid current is around 3.6%.

The power delivered to MES stack and also the voltage across of the stack are shown in Fig. 9, in which both ISCs have an acceptable transient response and zero steady state error. It can be seen that with a proper change in the voltage applied to the MES, the power of MES is also changed. The closed-loop control for power, based on changing of the short-through duty cycle, tracks accurately the reference power for both Z-SN and Trans Z-SN.

The voltages of the capacitors of ZSNs 'V_c ' are shown in Fig. 10, in which Z-source converter has a better response than Trans Z-converter because the value of capacitor voltage overshoot during transient is smaller. However, as shown in Fig. 11, the DC link voltage 'V_{in}' of Trans Z-SN in the steady state is almost fixed compared to Z-SN. The price of inverter bridge semiconductors is directly related to DC link voltage so the cost and volume of Trans Z-source converter can be lower than Z-source converter because of it.

Short-through duty cycle D_0 of ICs are shown in Fig. 12, the value D_0 for Z-SN changes from 0.2 to 0.36 while for Trans Z-SN is around 0.12 for the whole simulation. Therefore, the range of output voltage variations and power delivered to MES is grater for Trans Z-SN.

B. *Comparison*

In this part of the paper, the proposed ICs are compared with classic IC using buck converter replacing the Z-source network, as shown in Fig. 13. In classic system, VSI is implemented to keep dc bus voltage constant, and buck converter supplies MES with the desired voltage.

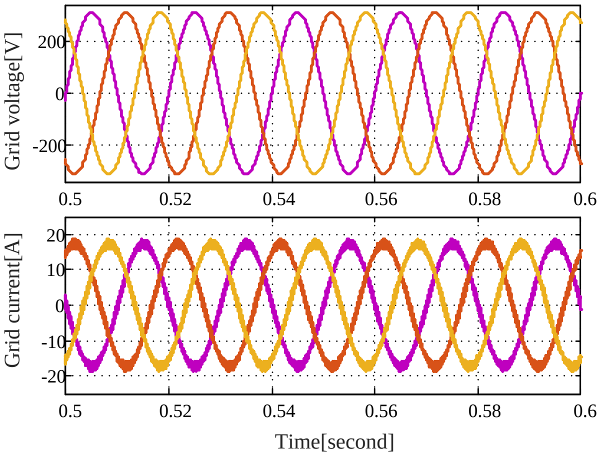

Fig. 8. Grid voltage and grid current.

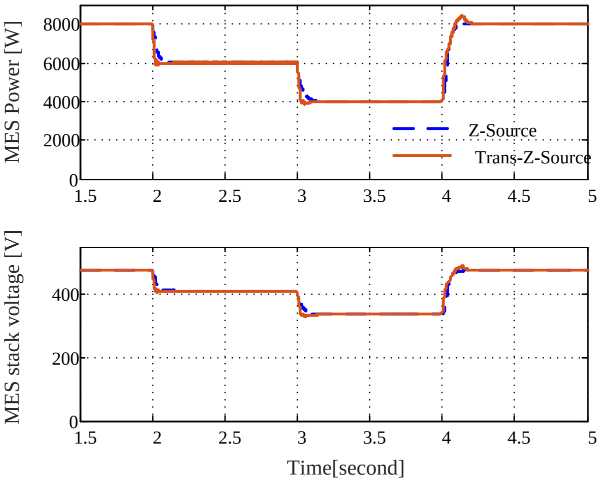

Fig. 9. MES power and MES voltage

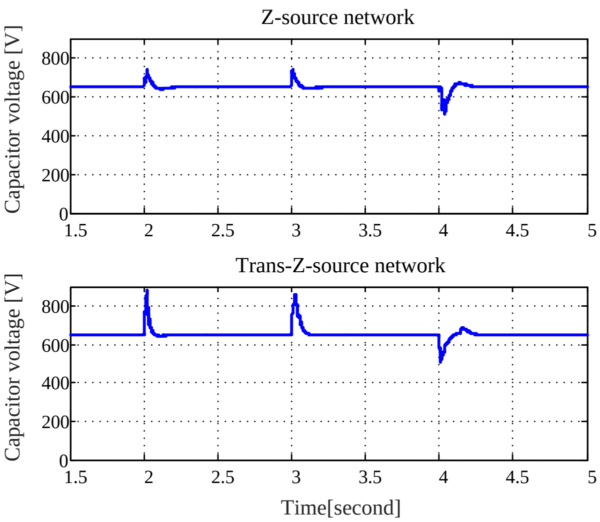

Fig. 10. Voltage of ZSN's capacitor

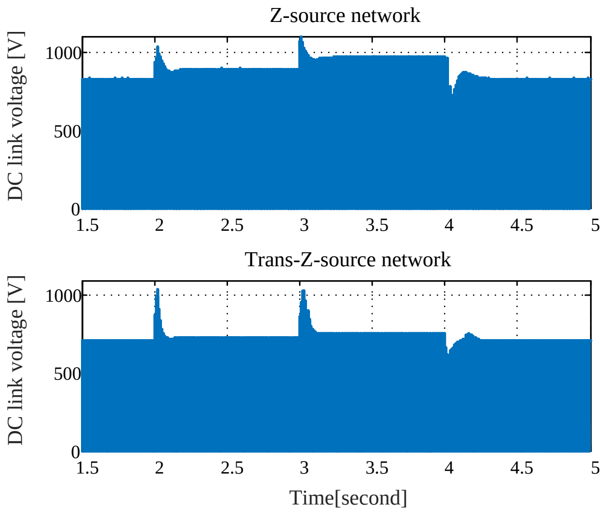

Fig. 11. DC link Voltage.

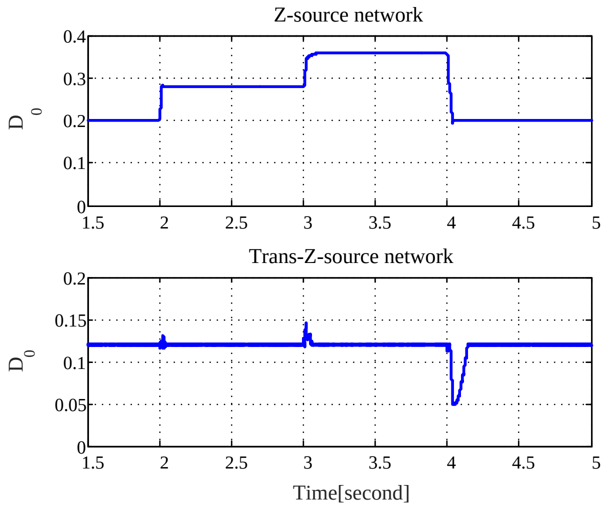

Fig. 12. Short-through duty cycle of ICs .

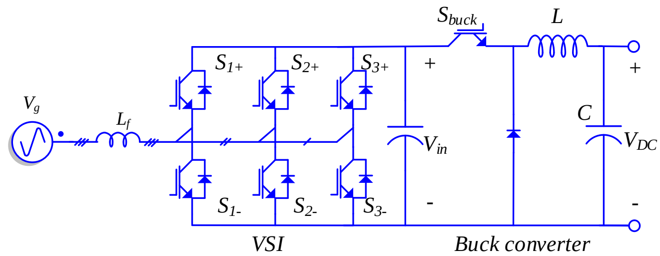

Fig. 13. Classic interlinking converter.

1) TSDP: The total switching device power (TSDP) can be used for evaluation of rating of converters. TSDP is calculated as [18]:

$$\text{TSDP} = \sum_{j=1}^{N} C_j V_{sj} I_{sj}, \tag{17}$$

where N is the number of semiconductors. C_j is cost factor, and it is defined as 1 for switches switch an 0.5 for diodes. I_{sj} and V_{sj} are current stress and voltage stress of semiconductor, respectively. Table II shows TSDP of different interlinking converters. It can be concluded that TSDP of proposed ICs is bigger than the classic system.

3) Number of components: In table. 2, the numbers of components of ICs are listed. It can be seen that classic system has one diode more than the others. ZSI needs to three inductors and capacitors while classic system needs one inductor and two capacitors, Trans Z-SN does not need to inductor but magnetizing inductor of its transformer is exactly the same as the other inductors, therefore its transformer can be considered as one inductor.

It can be concluded that Trans- Z-SN has the minimum number of components, and Z-SN has the maximum number of components.

3) plug-and-play capability: in ICs based on Z-SN and Trans-Z-SN, the MES can connect and disconnect by switch S_b, however, it is not possible for the classic system and it needs to another switch to do this task.

Table 2 Numbers of components and TSDP of ICs

Parameter	Classic System	Z-SN	Trans Z-SN
Switch	1	1	1
Diode	1	0	0
Inductor	1	2	0
Capacitor	2	3	2
Transformer	0	0	1
TSDP	90580	121690	123310

V. Conclusion

In this paper, an interlinking converter based ISCs was introduced for MES stack. ISC principles of operation were surveyed and an appropriate control method was suggested for application of ISC as a power conditioner in an MES connected to the three-phase grid. The control method employs two control loops for absorbing active/reactive powers, low current THD, and ISC capacitor voltage regulation. Obtained simulation results in MATLAB/Simulink are presented to verify the performance of the ICs. From obtained results, it can be concluded that Trans Z-source converter is the best IC due to 1) it has a good response in AC and DC sides, 2) MES can be supplied with a wide range of voltage, 3) it has the minimum numbers of components.

Acknowledgment

The research leading to these results has received funding from the European Union’s Horizon 2020 research and innovation programme under the Marie Skłodowska-Curie grant agreement No 712949 (TECNIOspring PLUS) and from the Agency for Business Competitiveness of the Government of Catalonia.

Also, this work has been supported by the Spanish Ministry of Economy and Competitiveness under the projects ENE2016-79493-R and ENE2017-88889-C2-1-R. Any opinions, findings and conclusions or recommendations expressed in this material are those of the authors and do not necessarily reflect those of the host institutions or funders.

References

[1] N. Bashir, B. Modu, and P. Harcourt, “Techno-Economic Analysis of Off-grid Renewable Energy Systems for Rural Electrification in North- eastern Nigeria,” vol. 8, no. 3, 2018.

[2] D. H. Mojonero, A. R. Villacorta, and J. L. Kuong, “Impact Assessment of Net Metering for Residential Photovoltaic Distributed Generation in Peru,” vol. 8, no. 3, 2018.

[3] M. Shahparasti, M. Mohamadian, P. T. Baboli and A. Yazdian, "Toward Power Quality Management in Hybrid AC–DC Microgrid Using LTC-L Utility Interactive Inverter: Load Voltage–Grid Current Tradeoff," in *IEEE Transactions on Smart Grid*, vol. 8, no. 2, pp. 857-867, March 2017

[4] D. Remon, W. Zhang, A. Luna, I. Candela and P. Rodriguez, "Grid Synchronization of Renewable Generation Systems Using Synchronous Power Controllers," *2017 IEEE 6th International Conference on Renewable Energy Research and Applications (ICRERA)*, San Diego, CA, 2017, pp. 169-174.

[5] M. Shahparasti, M. Mohamadian, P. T. Baboli and A. Yazdian, "Toward Power Quality Management in Hybrid AC–DC Microgrid Using LTC-L Utility Interactive Inverter: Load Voltage–Grid Current Tradeoff," in *IEEE Transactions on Smart Grid*, vol. 8, no. 2, pp. 857-867, March 2017

[6] M. Abdollahi, J. I. Candela, J. Rocabert, R. S. M. Aguilar and P. Rodriguez, "Generation frequency support by renewable SSG SPC unit on interconnected areas," *2017 IEEE 6th International Conference on Renewable Energy Research and Applications (ICRERA)*, San Diego, CA, 2017, pp. 977-982.

[7] G. Morales-España, R. Baldick, J. García-González and A. Ramos, "Power-Capacity and Ramp-Capability Reserves for Wind Integration in Power-Based UC," in *IEEE Transactions on Sustainable Energy*, vol. 7, no. 2, pp. 614-624, April 2016.

[8] Y. Zhang, S. Shen and J. L. Mathieu, "Distributionally Robust Chance-Constrained Optimal Power Flow With Uncertain Renewables and Uncertain Reserves Provided by Loads," in *IEEE Transactions on Power Systems*, vol. 32, no. 2, pp. 1378-1388, March 2017.

[9] D. Alkano and J. Scherpen, "Distributed supply coordination for Power-to-Gas facilities embedded in energy grids," in *IEEE Transactions on Smart Grid*, vol. PP, no. 99, pp. 1-1.

[10] S. Clegg and P. Mancarella, "Storing renewables in the gas network: modelling of power-to-gas seasonal storage flexibility in low-carbon power systems," in *IET Generation, Transmission & Distribution*, vol. 10, no. 3, pp. 566-575, 2 18 2016.

[11] Y. Li, W. Liu, M. Shahidehpour, F. Wen, K. Wang and Y. Huang, "Optimal Operation Strategy for Integrated Natural Gas Generating Unit and Power-to-Gas Conversion Facilities," in *IEEE Transactions on Sustainable Energy*, vol. 9, no. 4, pp. 1870-1879, Oct. 2018.

[12] D. Jiandong and J. Zhuanting, "Research on improving flexibility of integrated power and gas energy system considering P2G and demand response," *2017 IEEE Conference on Energy Internet and Energy System Integration (EI2)*, Beijing, 2017, pp. 1-6.

[13] D. A. Jadhav, S. Ghosh Ray, and M. M. Ghangrekar, “Third generation in bio-electrochemical system research – A systematic review on mechanisms for recovery of valuable by-products from wastewater,” *Renew. Sustain. Energy Rev.*, vol. 76, no. March, pp. 1022–1031, 2017.

[14] Y. P. Siwakoti, F. Z. Peng, F. Blaabjerg, P. C. Loh, and G. E. Town, “Impedance-source networks for electric power conversion Part I: A topological review,” *IEEE Trans. Power Electron.*, vol. 30, no. 2, pp. 699–716, 2015.

[15] K. P. Nevin, T. L. Woodard, A. E. Franks, Z. M. Summers, and D. R. Lovley, “Microbial Electrosynthesis: Feeding Microbes Electricity To Convert Carbon Dioxide and Water to Multicarbon Extracellular Organic Compounds,” *MBio*, vol. 1, no. 2, Jun. 2010.

[16] J. Sadhukhan *et al.*, “A critical review of integration analysis of microbial electrosynthesis (MES) systems with waste biorefineries for the production of biofuel and chemical from reuse of CO2,” *Renew. Sustain. Energy Rev.*, vol. 56, pp. 116–132, 2016.

[17] P. Rodríguez, A. Luna, I. Candela, R. Mujal, R. Teodorescu, and F. Blaabjerg, “Multiresonant frequency-locked loop for grid synchronization of power converters under distorted grid conditions,” *IEEE Trans. Ind. Electron.*, vol. 58, no. 1, pp. 127–138, 2011

[18] S. Dehghan, M. Mohamadian, and a. Y. Varjani, “A New Variable-Speed Wind Energy Conversion System Using Permanent-Magnet Synchronous Generator and Z-Source Inverter,” *Energy Conversion, IEEE Trans.*, vol. 24, no. 3, pp. 714–724, 2009.

[19] R. Muñoz-Aguilar, D. Molognoni, P. Bosch-Jimenez, E. Borràs, M. Della Pirriera, and Á. Luna, “Design, Operation, Modeling and Grid Integration of Power-to-Gas Bioelectrochemical Systems,” *Energies*, vol. 11, no. 8, p. 1947, Jul. 2018.